


# Comprehensive analysis of mutations of renal cell carcinoma in an autosomal dominant polycystic kidney disease patient

Kwang Eon Shim, MD<sup>a</sup>, Chung Lee, PhD<sup>b</sup>, Jin Up Kim, MD<sup>a</sup>, Gwang Ho Choi, MD<sup>a</sup>, Kyoung Min Kwak, MD<sup>a</sup>, Seok Hyung Kim, PhD<sup>a</sup>, Hyunho Kim, PhD<sup>c</sup>, Jong Woo Yoon, PhD<sup>a</sup>, Tae Young Shin, MD<sup>d</sup>, Chang Wook Jeong, PhD<sup>e</sup>, Hyunsuk Kim, PhD<sup>a,\*</sup> 

## Abstract

Renal cell carcinoma (RCC) is known to be more prevalent in autosomal dominant polycystic kidney disease (ADPKD) patients than in the general population. However, little is known about genetic alterations or changes in signaling pathways in RCC in patients with ADPKD.

In the current report, whole-exome and transcriptome sequencing was performed for paired samples of tumor tissue, cyst tissue, and peripheral blood (triple set) from a patient diagnosed with ADPKD and RCC.

A 68-year-old man with ADPKD underwent left partial nephrectomy and was diagnosed with RCC. DNA and RNA were extracted from the triple set of the patient. A nonsense mutation in *PKD2* (p.Arg742X), which is well known as a pathogenic variant in ADPKD, was identified in the paired triple set. In the tumor sample, a somatic missense mutation of *VHL* (p.S65L) was found, which is known as a pathogenic mutation in Von Hippel-Lindau syndrome and RCC. Furthermore, loss of chromosome 3p, where *VHL* is located, was detected. Upregulated VEGFA was found in the analysis of RCC mRNA, which might be caused by the loss of *VHL* and accelerate angiogenesis in RCC.

Proliferation was also expected to be activated by the MAPK signaling pathway, including *NRAS* and *MAPK1* expression.

**Abbreviations:** 3p = chromosome 3, ADPKD = autosomal dominant polycystic kidney disease, AP-1 = activator protein-1, ccRCC = clear cell renal cell carcinoma, COSMIC = Catalogue of Somatic Mutations in Cancer, CT = computed tomography, DEG = differentially expressed gene, ExAC = Exome Aggregation Consortium, FDR = false discovery rate, FPKM = fragments per kilobase of exon per million fragments mapped, GATK = Genome Analysis Tool Kit, GO = Gene Ontology, GPCRs = G-coupled protein receptors, GSEA = gene set enrichment analyses, KEGG = Kyoto Encyclopedia of Genes and Genomes, MAPK = mitogen-activated protein kinase, mTOR = mammalian target of rapamycin, RCC = renal cell carcinoma, SCNAs = somatic copy number alterations, VAFs = variant allele fractions, VHL = Von Hippel-Lindau.

**Keywords:** autosomal dominant polycystic kidney disease (ADPKD), MAPK signaling pathway, renal cell carcinoma (RCC), VHL

Editor: Muhammed Mubarak.

KES and CL contributed equally to this work.

Data Availability Statement: All produced data are available as Supplementary Information online.

This research was supported by a grant of the National Research Foundation of Korea (grant number: NRF-2016R1D1A1B03934173 and NRF-2016R1A2B4015516) and the Hallym University Research Fund 2017 (HURF-2017-55). This research was financially supported by the Ministry of Trade, Industry and Energy (MOTIE) and Korea Institute for Advancement of Technology (KIAT) through the National Innovation Cluster R&D program (P0006662\_Development of monitoring system using markers related to metabolic diseases).

The authors have no conflicts of interest to disclose.

Supplemental Digital Content is available for this article.

All data generated or analyzed during this study are included in this published article [and its supplementary information files];

<sup>a</sup> Internal Medicine, Hallym University Medical Center, Chuncheon Sacred Heart Hospital, Chuncheon-si, Gangwon-do, Republic of Korea, <sup>b</sup> Samsung Genome Institute, Samsung Medical Center, Seoul, <sup>c</sup> Center for Medical Innovation, Seoul National University Hospital, Seoul, <sup>d</sup> Urology, 24253, Hallym University Medical Center, Chuncheon Sacred Heart Hospital, Chuncheon-si, Gangwon-do, <sup>e</sup> Urology, Seoul National University Hospital, Seoul, Republic of Korea.

\* Correspondence: Hyunsuk Kim, Internal Medicine, Hallym University Medical Center, Chuncheon Sacred Heart Hospital, Chuncheon-si, Gangwon-do, 24253, Republic of Korea (e-mail: nephrokim@hallym.or.kr).

Copyright © 2020 the Author(s). Published by Wolters Kluwer Health, Inc.

This is an open access article distributed under the terms of the Creative Commons Attribution-Non Commercial License 4.0 (CCBY-NC), where it is permissible to download, share, remix, transform, and buildup the work provided it is properly cited. The work cannot be used commercially without permission from the journal.

How to cite this article: Shim KE, Lee C, Kim JU, Choi GH, Kwak KM, Kim SH, Kim H, Yoon JW, Shin TY, Jeong CW, Kim H. Comprehensive analysis of mutations of renal cell carcinoma in an autosomal dominant polycystic kidney disease patient. *Medicine* 2020;99:19(e20071).

Received: 21 October 2019 / Received in final form: 10 March 2020 / Accepted: 1 April 2020

<http://dx.doi.org/10.1097/MD.00000000000020071>

## 1. Introduction

Autosomal dominant polycystic kidney disease (ADPKD) is a hereditary disorder of the kidneys characterized by markedly enlarged kidneys with extensive cyst formation throughout. As kidney function diminishes with age, these cysts progressively enlarge.<sup>[1]</sup> ADPKD is a systemic disorder, and cysts appear in the kidneys, liver, pancreas, brain, spleen, ovaries, and testes. Other disorders associated with ADPKD include inguinal and abdominal hernias, cardiac valvular disorders, and aneurysms of coronary arteries, the aorta, and cerebral arteries.<sup>[2]</sup>

The prevalence of renal cell carcinoma (RCC) in patients with ADPKD is known to be high.<sup>[3]</sup> Whether this is due to chronic dialysis or the underlying disease is still speculative, but attending physicians should be aware of the malignant potential of ADPKD, especially in patients receiving concomitant dialysis.<sup>[4]</sup> The most common histological types of kidney tumors are clear cell RCC (ccRCC, 75%), type I papillary RCC (5%), type II papillary RCC (10%), and chromophobe RCC and oncocytoma (10%).<sup>[5]</sup>

Meanwhile, many reports have described genetic alterations in RCC. In roughly 95% of ccRCC cases, the short arm of chromosome 3 (3p) is lost; therefore, loss of 3p is the most frequent genetic alteration linked to ccRCC development. Gain of 5q (occurring in 69% of cases), partial loss of 14q (occurring in 42% of cases), gain of 7q (occurring in 20% of cases), loss of 8p (occurring in 32% of cases), and deletion of 9p (occurring in 29% of cases) are less frequent in ccRCC than loss of 3p, but are nonetheless important genetic alterations in ccRCC. On the level of genes, *MTOR 1*, *8*, *KDM5C*, *BAP-1*, *SETD2*, *PBRM-1*, and *VHL* have been linked to the pathogenesis of ccRCC.<sup>[6]</sup> However, the pathogenic gene alterations in RCC occurring in patients with ADPKD are poorly understood.

G-coupled protein receptors (GPCRs) and Wnt/  $\beta$ -catenin signaling are among the numerous signaling pathways that appear to be involved in ADPKD, as are mammalian target of rapamycin (mTOR), B-Raf/ERK, mitogen-activated protein kinase (MAPK), activator protein-1 (AP-1) transcription factor, RKIP, and second messengers including  $Ca^{2+}$  and cAMP.<sup>[7]</sup> Nonetheless, little is known about changes in signaling pathways in RCC in patients with ADPKD.

However, there was a report of dysregulation of catenin signaling in RCC in a patient with Von Hippel-Lindau (VHL) syndrome, which also predisposes patients to the development of polycystic kidney disease, like ADPKD. That study suggested that disruption of this signaling pathway may be the link between RCC and polycystic kidney disease.<sup>[8]</sup>

We conducted a comprehensive analysis based on whole exome and transcriptome sequencing using blood, cyst, and RCC tissue obtained from an ADPKD patient. Through this analysis, we attempted to identify specific genetic alterations and changes in signaling pathways in RCC in a patient with ADPKD.

## 2. Materials and methods

### 2.1. Patient

A 68-year-old male ADPKD patient presented to a tertiary hospital for treatment of a left renal mass that was incidentally detected on a computed tomography (CT) scan. An early enhanced-washout nodule measuring  $2.4 \times 2.7 \times 2.7$  cm was seen in the left kidney interpolar area, and was suspected to be RCC with no involvement of other adjacent organs or lymph nodes

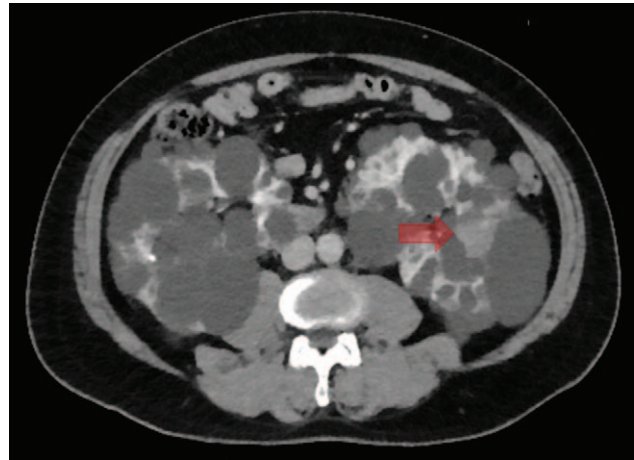


**Figure 1.** Renal cell carcinoma measuring  $2.4 \times 2.7 \times 2.7$  cm in the left kidney on a CT scan. An early enhanced-washout mass measuring  $2.4 \times 2.7 \times 2.7$  cm was found on abdominopelvic CT in the left kidney interpolar area and was suspected to be renal cell carcinoma.

(Fig. 1). The decision was made to perform left partial nephrectomy, and the patient was admitted to the urology department.

After surgery, an RCC with a negative margin was identified from the intraoperative frozen section biopsy (Fig. 2). The final pathological diagnosis was ccRCC.

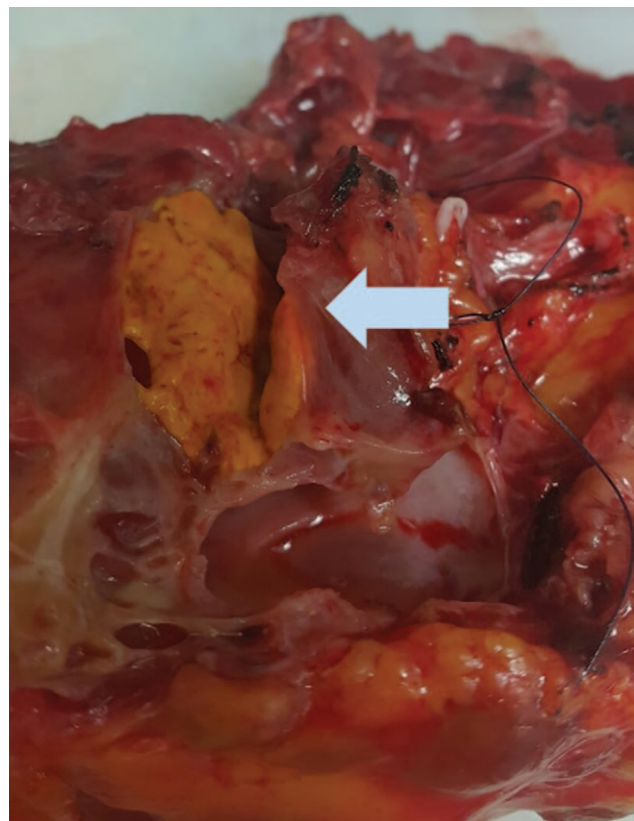


**Figure 2.** Renal cell carcinoma measuring 2.7 cm. The patient underwent partial nephrectomy and margin-negative renal cell carcinoma was confirmed from the frozen section biopsy. The final pathological diagnosis was clear cell RCC.

The study protocol was approved by the Institutional Review Board of Chuncheon Sacred Heart Hospital (IRB number CHUNCHEON 2017-11-106-008). The study protocol conformed to ethical guidelines of the World Medical Association Declaration of Helsinki.

## 2.2. Whole exome sequencing and analysis

Genomic DNA was extracted from the peripheral blood of the patient and from the cyst and tumor tissue of the removed kidney, and exome regions were captured in each sample using Agilent's SureSelect Human All Exon V5-post (Agilent Technologies, Santa Clara, CA). Exome sequencing was performed on an Illumina HiSeq 2500 platform (Illumina, San Diego, CA). Sequencing reads were aligned to the hg19 reference genome with the Burrows-Wheeler Aligner v0.7.5,<sup>[9]</sup> using the MEM algorithm. The aligned reads were processed, with sorting, de-duplication, local realignment, and base recalibration performed using SAMtools v1.2,<sup>[10]</sup> Picard tools v1.127 (<https://broadinstitute.github.io/picard/>), and the Genome Analysis Tool Kit (GATK) v3.8,<sup>[11]</sup> respectively (Fig. 3A).

Germline or somatic variants, including single-nucleotide variants, insertions, and deletions, were called by the haplotype caller of GATK, MuTect2,<sup>[12]</sup> VarScan v2.3.6,<sup>[13]</sup> and Pindel v0.2.5a4,<sup>[14]</sup> and annotated minor allele frequency and clinical information were obtained from public databases, such as the Catalogue of Somatic Mutations in Cancer (COSMIC), Exome Aggregation Consortium (ExAC), the 1000 Genomes Project (1000G), and ClinVar, as well as prediction tools such as SIFT, PolyPhen-2, MutationTaster, and GERP++ by ANNOVAR.<sup>[15]</sup> Structural variants and copy number alterations were calculated by an in-house method (referred to as JuLI) and EXCAVATOR<sup>[16]</sup> in paired mode, respectively (Fig. 4). Detected variants were prioritized as previously described (submitted).

## 2.3. Whole transcriptome sequencing and analysis

mRNA isolated from peripheral blood and cyst and tumor tissue was processed, captured using the TruSeq RNA Access Library (Illumina, San Diego, CA), and sequenced on the HiSeq 2500 platform (Illumina, San Diego, CA). RNA sequencing reads were aligned to hg19 in the default mode of Tophat v2.0.13.<sup>[17]</sup> The aligned reads were assembled to known or novel transcripts using the RABT algorithm in Cufflinks v2.2.1.<sup>[18]</sup> Possible fusion genes were predicted using the clustering method of spanning reads and split reads and the heuristic filter of deFuse 0.6.2 (Fig. 3B).<sup>[19]</sup>

To identify mutations at the transcriptome level, RNA sequencing reads were mapped to hg19 with STAR v2.4.0f1.<sup>[20]</sup> Aligned reads were marked as duplicates, trimmed adaptor sequences, indel realignment, and base recalibration using Trimmomatic v0.32,<sup>[21]</sup> as well as SAMtools, Picard tools, and GATK as described above. Variants were called using the haplotype caller of GATK.

Aligned RNA-Seq reads were calculated as fragments per kilobase of exon per million fragments mapped (FPKM) at the gene or transcript level. After a quality control process that involved filtering out zero-count genes, logarithm-2-based transformation, and quantile normalization, a differentially expressed gene (DEG) analysis of 18,633 genes was performed between the tumor samples and normal blood, and 3284 genes showed a significant differential expression pattern, as indicated by an absolute fold change above 2. We performed gene set

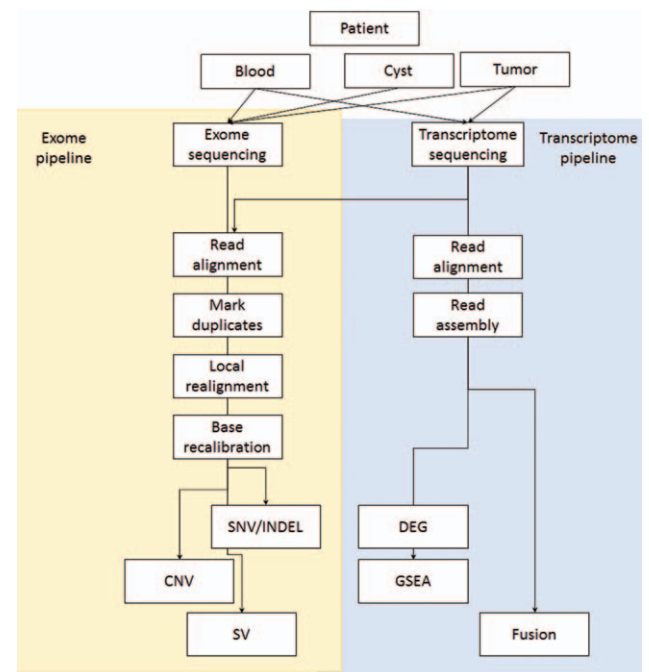


**Figure 3.** WES and WTS pipeline. (A) Genomic DNA was extracted and exome regions were captured in each sample. The aligned reads were processed, with sorting, de-duplication, local realignment, and base recalibration performed. (B) mRNA was isolated, captured, sequenced, and aligned. The aligned reads were assembled to known or novel transcripts. Possible fusion genes were predicted. CNV=copy number variation, INDEL=insertions, and deletions, SNV=single-nucleotide variants, SV=structural variants, WES and WTS=whole exome sequencing and whole transcriptome sequencing and analysis.

enrichment analyses (GSEA)<sup>[22,23]</sup> to identify significant patterns of differential expression in Kyoto Encyclopedia of Genes and Genomes (KEGG)<sup>[24]</sup> pathways and in Gene Ontology (GO).<sup>[25,26]</sup> We set the significance threshold as a false discovery rate (FDR) below 0.05.

## 3. Results

### 3.1. Causal germline mutation of ADPKD

To diagnose ADPKD, we examined the sequences of *PKD1* and *PKD2* from the blood samples, and detected a nonsense *PKD2* mutation, R742X, which is well known as a definitely pathogenic variant in ADPKD.<sup>[27]</sup> In a functional study, it was found that this nonsense *PKD2* mutation results in an absence of the C-terminal region containing the coiled-coil domain, which causes failure to create the polycystin-1 and polycystin-2 complex that regulates Ca<sup>2+</sup>, Na<sup>+</sup>, and K<sup>+</sup> concentration as a Ca<sup>2+</sup>-regulated non-selective cation channel in renal epithelial cells.<sup>[28]</sup>

### 3.2. Germline and somatic mutations of RCC

We performed whole exome sequencing for paired samples of tumor tissue, cyst tissue, and peripheral blood from the patient, and identified germline and somatic mutations in the blood and tumor tissues. First, we found several germline and somatic mutations in genes including *DNAH5*, *KMT5A*, *CCDC175*, and *TPSAB1* from the blood, tumor, and cyst of the patient (Table 1). Next, we investigated mutations in known oncogenes and tumor suppressor genes in RCC. In particular, eight of 19 genes (*VHL*,

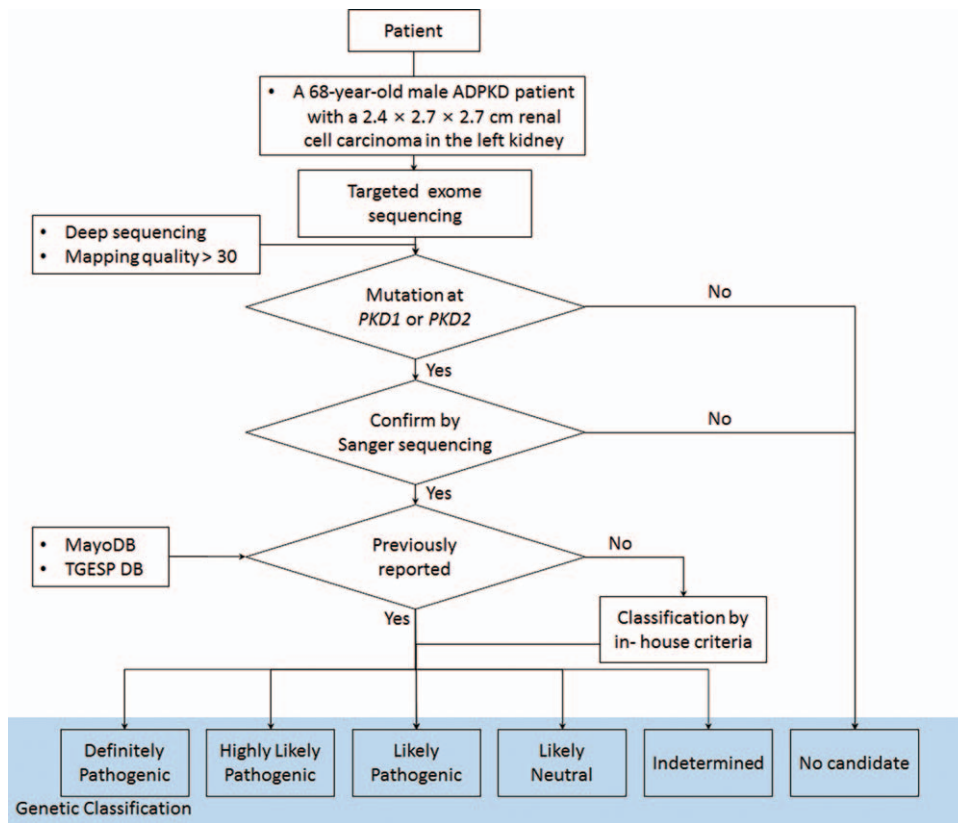


**Figure 4.** Variant calling and analysis pipeline by *Targeted exome sequencing*. Germline or somatic variants, including single-nucleotide variants, insertions, and deletions, were called and annotated minor allele frequency and clinical information. A previously reported database was referenced and the variants were classified into 6 categories.

*PBRM1*, *SETD2*, *KDM5C*, *PTEN*, *BAP1*, *MTOR*, and *TP53*) were found to be extremely significantly mutated (FDR < 0.1 and  $q < 0.00001$ ) in RCC in a previous study.<sup>[29]</sup> In this case, a missense *VHL* mutation, S65L, which has been reported to lead to tumorigenesis by disrupting the dynamic organization of pVHL and HIF-1 $\alpha$  for ubiquitin-dependent degradation,<sup>[30]</sup> was only detected in tumor tissue, not blood or cyst samples (Table 1). Furthermore, a novel missense *SMARCA4* mutation (K981T) was also detected. *SMARCA4* is a known tumor suppressor that encodes BRG1, which is an ATPase enzymatic subunit of the switch/sucrose non-fermentable (SWI/SNF) chromatin remodeling complex in RCC.

**3.3. Somatic copy number alterations of RCC**

The global characterization of somatic copy number alterations (SCNAs) in RCC was previously analyzed, and it was found that SCNAs occurred at fewer sites in RCC than in other cancers, and that more SCNAs involved whole chromosomes or arm-level alterations than focal events. Frequent patterns of SCNAs in RCC were found to include loss of chromosome 3p and 14q or gain of chromosome 5q at the arm level, as well as gain of 5q35, 8q24, 3q26, and 1q32 or loss of 14q24, 9p21.3, 6q26, 8p11, 10q23, 1p36, 4q35, 13q21, 15q21, and 2q37 at the focal level.<sup>[29]</sup> Based on these previous studies, we analyzed SCNAs using EXCAVATOR in paired-end mode between blood and tumor whole exome

**Table 1**  
**Germline and somatic mutations in an ADPKD patient with RCC.**

Gene	Blood	Tumor	Cyst	Nucleotide	AA	Chr	Mutation type
<i>DNAH5</i>	No variant	Heterozygous	No variant	c.G9913A	p.D3305N	chr5	Somatic
<i>DNAH5</i>	Heterozygous	Heterozygous	Heterozygous	c.G7634A	p.R2545H	chr5	Germline
<i>KMT5A</i>	No variant	Heterozygous	Heterozygous	c.C179T	p.P60L	chr12	Somatic
<i>KMT5A</i>	Heterozygous	Heterozygous	Heterozygous	c.A362G	p.K121R	chr12	Germline
<i>KMT5A</i>	Heterozygous	Heterozygous	Heterozygous	c.G364C	p.G122R	chr12	Germline
<i>KMT5A</i>	No variant	Heterozygous	Heterozygous	c.A464C	p.Q155P	chr12	Somatic
<i>CCDC175</i>	No variant	Heterozygous	No variant	c.G1762T	p.A588S	chr14	Somatic
<i>CCDC175</i>	Heterozygous	Heterozygous	Heterozygous	c.A1715G	p.Y572C	chr14	Germline
<i>TPSAB1</i>	No variant	Heterozygous	Heterozygous	c.C422T	p.T141I	chr16	Somatic
<i>TPSAB1</i>	Heterozygous	Heterozygous	Heterozygous	c.C508T	p.P170S	chr16	Germline
<i>VHL</i>	No variant	Heterozygous	No variant	c.C194T	p.S65L	chr3	Somatic
<i>SMARCA4</i>	No variant	Heterozygous	No variant	c.A2942C	p.K981T	chr19	Somatic

**Table 2**  
Somatic copy number variants detected in paired tumor-cyst samples.

Chromosome	Start	End	Cytoband	Segment	CNF	CN	Call	ProbCall
chr1	145487231	157551538	1q21-q23.1	0.3548108	2.557636	3	1	0.971637
chr3	239350	87325637	3p	-0.5913577	1.327436	1	-1	0.999962
chr7	193220	4845426	7p22.2-22.3	0.38345534	2.608925	3	1	0.990431
chr13	43358174	43566290	13q14.11	0.37740844	2.598013	3	1	0.99304
chr13	110866089	115091802	13q34	0.36531107	2.576319	3	1	0.991095

CN=cop number, CNF=cop number fraction, ProbCall=probability of call.

sequencing. First, loss of chromosome 3p, which is the most commonly involved pattern (frequency: 95% in ccRCC) at the arm level, was detected. This region contains *VHL*, where a missense mutation, S65L, was detected in this patient's tumor, as well as *PBRM1*, *BAP1*, *SETD2*, and *CADM2*, which are known to be the most frequently mutated genes in RCC, as described above, and are putative tumor suppressor genes. Next, gain of 1q21-23.1, 7p22.2-22.3, 13q14.11, and 13q34 at the focal level, which is not a known pattern in RCC, was detected (Table 2). Taken together, we found that double somatic mutations—the missense mutation S65L and the loss of chromosome 3p—occurred at *VHL*, a tumor suppressor gene, in the tumor tissue of the ADPKD patient. The loss of function of *VHL* might have influenced the development of RCC in this ADPKD patient.

Since tumor purity was calculated as about 60% by our in-house method, we were able to determine the normalized variant allele fractions (VAFs) of each genotype of somatic mutations. The loss-of-heterozygosity of the *VHL* mutation was called as a heterozygous variant with 45% VAF, which was normalized to 100% VAF with the loss of chromosome 3p, where *VHL* is located.

### 3.4. RNA expression patterns in the patient

Gene set enrichment analyses (GSEA) detected significance in Kyoto Encyclopedia of Genes and Genomes (KEGG) pathway 255 and for Gene Ontology (GO) term 4475 (Supplementary Tables 1, <http://links.lww.com/MD/E151> and 2, <http://links.lww.com/MD/E151>). Especially, metabolic pathways, focal adhesion, the PI3K-Akt signaling pathway, and cancer pathways were the top-ranked pathways ordered by false discovery rate (FDR). Additionally, the RCC included 14 genes reported to be significantly differentially expressed in tumors in the KEGG database. Specifically, angiogenesis in tumors seemed to be upregulated through the VEGF signaling pathway resulting from the loss of *VHL*. Moreover, proliferation was expected to be activated by the MAPK signaling pathway, including *NRAS* and *MAPK1* expression (Supplementary Table 2, <http://links.lww.com/MD/E151>).

## 4. Discussion

In the present study, we found loss of function of the *VHL* gene, including 3p deletion combined with a missense mutation in RCC, in a patient with ADPKD, not VHL syndrome. The causal mutation of ADPKD was a PKD2 truncating mutation. We also found several germline and somatic mutations, including *SMARCA4* (K981T), a novel missense mutation. In the transcriptome analysis, we found that angiogenesis seemed to be accelerated through the upregulation of the VEGF signaling pathway in RCC.

In this study, we investigated the mRNA expression of genes related to RCC and found that several genes were upregulated or downregulated. In this case, angiogenesis might have been activated by the VEGF pathway. VEGF binding to its receptor leads to signaling via the PI3K/AKT, Raf/MAPK, PLC, and Src pathways, resulting in increased cell permeability, endothelial cell proliferation, migration, and survival through angiogenesis. VEGF expression in cancer is elevated in response to tissue hypoxia, as a result of mutations of the *VHL* gene. It is known that HIF1, which activates VEGF, is degraded by the *VHL* gene product.<sup>[30]</sup> In the case described in the present study, the possibility of overexpression of VEGF by HIF1, which was not degraded due to the loss of function of *VHL*, can be considered. In addition, TGF- $\alpha$  can accelerate tumorigenesis through cell proliferation, and TGF- $\beta$  is known to induce apoptosis and differentiation. In this study, TGF- $\alpha$  was upregulated in the tumor and TGF- $\beta$  was downregulated, which might have caused RCC.

*VHL* syndrome is a neoplastic disorder inherited in an autosomal dominant manner that manifests through tumor development in a broad range of tissues, including the kidneys, adrenal glands, pancreas, inner ear, retina, spine, and cerebellum. The bilateral multifocal renal tumors that can occur in association with *VHL* syndrome are malignant and capable of metastasis. The risk posed by such tumors is underscored by the fact that in the past, as many of 40% of untreated patients with *VHL* syndrome died of advanced ccRCC. It is known that the frequency of sporadic RCC increases with loss of function of the *VHL* tumor suppressor gene in *VHL* syndrome. In this report, we showed a case of ccRCC caused by loss of function of the *VHL* gene, which co-existed with a PKD2 truncating mutation that was the causative gene of ADPKD.  $\beta$ -catenin is known to be the linkage between RCC and PKD. Similarly, VEGF may be a linkage between RCC and PKD, so further efforts should be made to elucidate the pathogenesis.

mTOR is considered to be the master regulator of cell growth. Upon receiving growth signals, mTOR promotes several anabolic processes in which macromolecules are synthesized, thereby increasing cellular biomass, and limits catabolic processes such as autophagy.<sup>[31]</sup> The mTOR signal pathway is dysregulated in some common types of cancer, including renal cancer, and abnormal activity of mTOR was shown in ADPKD. Taken together, the incidence of kidney cancer is closely associated with ADPKD.

Polycystin-1, the *PKD1* gene product, regulates G0/G1 of the cell cycle by serving as a regulator of the G1 checkpoint; thus, immature G1 exit occurs in ADPKD. It has also been found that oxidative stress plays a major role in ADPKD. Therefore, the occurrence of somatic mutations in ADPKD might be caused by immature G1 exit and DNA damage through oxidative stress.

A major strength of this study is that it presents the first finding of loss of function in the *VHL* gene in RCC in a patient with ADPKD. The primary limitation of this study is that in selected pathways, the mRNA dose was not equal to the protein expression dose. Therefore, experimental support of the upregulated pathway is needed.

## 5. Conclusion

In this study, we investigated a Korean ADPKD patient with RCC and found some somatic mutations in tumor suppressor genes and oncogenes using whole exome sequencing. In conclusion, loss of function of the *VHL* gene can be a causative genetic alteration in RCC with ADPKD. VEGF, mTOR, and oxidative stress could be accelerators of kidney cancer in patients with ADPKD.

## Author contributions

K.H.S., L.C and S.K.E conceived this study and drafted the manuscript. K.J.U, K.M.P, K.S.H and C.G.H helped collect the clinical samples. K.H.H and J.C.W helped to prepare clinical samples for sequencing. L.C. and K.H.S. carried out sequencing. Y.J.W. and S.T.Y. participated in the design of the study. K.H.S. contributed to revision and discussion of this study.

## References

- [1] Finnigan NA, Leslie SW. Polycystic kidney disease, adult [Internet]. Treasure Island (FL): StatPearls Publishing; 2019 [cited Sept 28, 2019]. Available from: <https://www.ncbi.nlm.nih.gov/books/NBK430685/>.
- [2] Martinez JR, Grantham JJ. Polycystic kidney disease: etiology, pathogenesis, and treatment. *Dis Mon* 1995;41:693–765.
- [3] Violo L, De Francesco M, Schoenholzer C. Risk of cancer in patients with polycystic kidney disease. *Lancet Oncol* 2016;17:e475.
- [4] Jilg CA, Drendel V, Bacher J, et al. Autosomal dominant polycystic kidney disease: prevalence of renal neoplasias in surgical kidney specimens. *Nephron Clin Pract* 2013;123:13–21.
- [5] Linehan WM, Grubb RL, Coleman JA, et al. The genetic basis of cancer of kidney cancer: implications for gene-specific clinical management. *BJU Int* 2005;95(Suppl 2):2–7.
- [6] Nabi S, Kessler ER, Bernard B, et al. Renal cell carcinoma: a review of biology and pathophysiology. *F1000Res* 2018;7:307.
- [7] Saigusa T, Bell PD. Molecular pathways and therapies in autosomal-dominant polycystic kidney disease. *Physiology (Bethesda)* 2015;30:195–207.
- [8] Peruzzi B, Bottaro DP. Beta-catenin signaling: linking renal cell carcinoma and polycystic kidney disease. *Cell Cycle* 2006;5:2839–41.
- [9] Li H, Durbin R. Fast and accurate short read alignment with Burrows-Wheeler transform. *Bioinformatics* 2009;25:1754–60.
- [10] Li H, Handsaker B, Wysoker A, et al. The sequence alignment/Map format and SAMtools. *Bioinformatics* 2009;25:2078–9.
- [11] McKenna A, Hanna M, Banks E, et al. The genome analysis Toolkit: a MapReduce framework for analyzing next-generation DNA sequencing data. *Genome Res* 2010;20:1297–303.
- [12] Cibulskis K, Lawrence MS, Carter SL, et al. Sensitive detection of somatic point mutations in impure and heterogeneous cancer samples. *Nat Biotechnol* 2013;31:213–9.
- [13] Koboldt DC, Zhang Q, Larson DE, et al. VarScan 2: somatic mutation and copy number alteration discovery in cancer by exome sequencing. *Genome Res* 2012;22:568–76.
- [14] Ye K, Schulz MH, Long Q, et al. Pindel: a pattern growth approach to detect break points of large deletions and medium sized insertions from paired-end short reads. *Bioinformatics* 2009;25:2865–71.
- [15] Wang K, Li M, Hakonarson H. ANNOVAR: functional annotation of genetic variants from high-throughput sequencing data. *Nucleic Acids Res* 2010;38:e164.
- [16] Magi A, Tattini L, Cifola I, et al. EXCAVATOR: detecting copy number variants from whole-exome sequencing data. *Genome Biol* 2013;14:R120.
- [17] Kim D, Pertea G, Trapnell C, et al. TopHat2: accurate alignment of transcriptomes in the presence of insertions, deletions and gene fusions. *Genome Biol* 2013;14:R36.
- [18] Trapnell C, Williams BA, Pertea G, et al. Transcript assembly and quantification by RNA-Seq reveals unannotated transcripts and isoform switching during cell differentiation. *Nat Biotechnol* 2010;28:511–5.
- [19] McPherson A, Hormozdiari F, Zayed A, et al. deFuse: an algorithm for gene fusion discovery in tumor RNA-Seq data. *PLoS Comput Biol* 2011;7:e1001138.
- [20] Dobin A, Davis CA, Schlesinger F, et al. STAR: ultrafast universal RNA-seq aligner. *Bioinformatics* 2013;29:15–21.
- [21] Bolger AM, Lohse M, Usadel B. Trimmomatic: a flexible trimmer for Illumina sequence data. *Bioinformatics* 2014;30:2114–20.
- [22] Mootha VK, Lindgren CM, Eriksson KF, et al. PGC-1 $\alpha$ -responsive genes involved in oxidative phosphorylation are coordinately down-regulated in human diabetes. *Nat Genet* 2003;34:267–73.
- [23] Subramanian A, Tamayo P, Mootha VK, et al. Gene set enrichment analysis: a knowledge-based approach for interpreting genome-wide expression profiles. *Proc Natl Acad Sci USA* 2005;102:15545–50.
- [24] Kanehisa M, Goto S. KEGG: Kyoto Encyclopedia of genes and genomes. *Nucleic Acids Res* 2000;28:27–30.
- [25] Gene Ontology Consortium. Gene Ontology Consortium: going forward. *Nucleic Acids Res* 2015;43(Database issue):D1049–56.
- [26] Ashburner M, Ball CA, Blake JA, et al. Gene ontology: tool for the unification of biology. The Gene Ontology Consortium. *Nat Genet* 2000;25:25–9.
- [27] Mochizuki T, Wu G, Hayashi T, et al. PKD2, a gene for polycystic kidney disease that encodes an integral membrane protein. *Science* 1996;272:1339–42.
- [28] Hanaoka K, Qian F, Boletta A, et al. Co-assembly of polycystin-1 and -2 produces unique cation-permeable currents. *Nature* 2000;408:990–4.
- [29] Cancer Genome Atlas Research Network. Comprehensive molecular characterization of clear cell renal cell carcinoma. *Nature* 2013;499:43–9.
- [30] Miller F, Kentsis A, Osman R, et al. Inactivation of VHL by tumorigenic mutations that disrupt dynamic coupling of the pVHL-hypoxia-inducible transcription factor-1 $\alpha$  complex. *J Biol Chem* 2005;280:7985–96.
- [31] Tee AR. The target of rapamycin and mechanisms of cell growth. *Int J Mol Sci* 2018;19:pii:E880.